Dispersive Electron Transport in tris(8-Hydroxyquinoline) Aluminum (Alq_3) Probed by Impedance Spectroscopy

Stefan Berleb and Wolfgang Brütting*
Experimental Physics II, University of Bayreuth, 95440 Bayreuth, Germany
(Received 10 June 2002; published 27 December 2002)

Electron transport in tris(8-hydroxyquinoline) aluminum (Alq_3) is investigated by impedance spectroscopy under conditions of space-charge limited conduction (SCLC). Existing SCLC models are extended to include the field dependence of the charge carrier mobility and energetically distributed trap states. The dipersive nature of electron transport is revealed by a frequency-dependent mobility with a dispersion parameter α in the range 0.4–0.5, independent of temperature. This indicates that positional rather than energetic disorder is the dominant mechanism for the dispersive transport of electrons in Alq_3.

DOI: 10.1103/PhysRevLett.89.286601 PACS numbers: 72.20.Ee, 73.50.–h, 73.61.Ph

The rapid progress in performance and lifetime make organic light-emitting diodes (OLEDs) suitable candidates for flat panel display applications. Since the first report of efficient and stable OLEDs [1] tris(8-hydroxyquinoline) aluminum (Alq_3) continues to be one of the most-widely used materials for OLEDs based on small molecules. Nevertheless, there is still a lack of understanding concerning the nature of electron transport in this material. On the one hand it was established from a variety of experiments that the electron mobility in Alq_3 shows a Poole-Frenkel–like dependence on the electric field typical for disordered organic semiconductors [2,3]. Additionally, time-of-flight (TOF) measurements gave clear evidence for dispersive hopping transport [4–6] (though recently nondispersive behavior under certain preparation conditions has been reported [7]). On the other hand, in a number of publications this field-dependent mobility was neglected and the dc transport was analyzed exclusively in terms of charge carrier trapping. Distributed trap states with energies ranging from the conduction level deep into the energy gap were identified as the current limiting factor in Alq_3 [8–10].

In principle, transient experiments like TOF can provide detailed information on the microscopic origin of charge transport in disordered materials. However, so far TOF studies have not been performed at different temperatures which is indispensable in order to clearly identify the underlying mechanism. An alternative approach to obtain such information in organic semiconductors is space-charge limited currents (SCLC) which can be observed when one contact is able to inject more carriers than the material has in thermal equilibrium [11,12]. These space charges not only determine the dc current-voltage (I-V) characteristics but also lead to a characteristic frequency-dependent electrical response [13], which can be used to get direct information on the dynamics of charge carriers. This method was successfully applied by Martens *et al.* to hole transport in the electroluminescent polymer poly(phenylenevinylene) (PPV) [14]. However, their approach was based on the assumption of a mobility independent of the electric field and the absence of trap states, both of which are known to significantly influence the electrical characteristics of Alq_3-based devices. In this Letter we therefore present a generalization of the model including a field-dependent mobility and the dynamics of trap states. We demonstrate that it allows one to distinguish between hopping transport and trapping of charge carriers.

The description of SCLC is based on the drift current equation and the Poisson equation (see, e.g., [15]). In the case of unipolar injection of electrons and band transport (ignoring diffusion) they read as

$$j(t) = qn(x,t)\mu F(x,t) + \varepsilon \frac{\partial F(x,t)}{\partial t}, \tag{1}$$

$$(\varepsilon/q)\frac{\partial F(x,t)}{\partial x} = n(x,t) + n_t(x,t), \tag{2}$$

where F denotes the electric field, n and n_t are the charge densities for free and trapped charges, respectively, q is the elementary charge, $\varepsilon = \varepsilon_r\varepsilon_0$ with the dielectric constant ε_r and the vacuum permittivity ε_0, and μ is the mobility of the charge carriers. The second term in the transport equation is the additional displacement current for the nonstationary situation.

In the case of dispersive hopping transport the diffusion equation has a non-Markovian form due to the time (respectively, frequency) dependence of the diffusion coefficient [16]. The same applies to the above given drift equation for the mobility. To circumvent the problem of an integro-differential equation in the time domain we directly formulate an expression for the frequency-dependent current $j(\omega)$. If we separate the stationary dc components from the frequency-dependent ac parts we obtain for the drift equation

$$\hat{j}_{ac}(\omega) + j_{dc} = q[n_{dc}(x) + \hat{n}_{ac}(x,\omega)]\mu_{dc}[F_{dc}(x)]\tilde{\mu}(\omega) \times [F_{dc}(x) + \hat{F}_{ac}(x,\omega)] + i\omega\hat{F}_{ac}(x,\omega), \tag{3}$$

where $\tilde{\mu}(\omega) = [1 + M(i\omega\tau_{\mathrm{tr}})^{1-\alpha}]$ contains the explicit frequency dependence of the hopping mobility [14] (τ_{tr} is the steady-state transit time of carriers). This kind of dependence is connected to the disordered nature of the materials reflecting the large spread of waiting times or hopping rates where α is a measure for the dispersivity ($\alpha = 1$ for nondispersive transport). Now the ac components are separated into amplitudes and phase factors ($e^{i\omega t}$) and Eq. (3) is developed to first order in the ac amplitudes (small signal analysis). From the dc components one obtains F_{dc} and thus the steady-state I-V characteristics [17]. The ac part F_{ac} yields the applied ac voltage $V_{\mathrm{ac}} = \int_0^d F_{\mathrm{ac}}(x)dx$ and from that one gets the complex admittance $\hat{Y} = A\,(\partial\hat{V}_{\mathrm{ac}}/\partial\hat{j}_{\mathrm{ac}})^{-1}$, where d and A are device thickness and area, respectively. $\hat{Y}$ is related to the experimentally observable quantities conductance G and capacitance C via $\hat{Y} = G + i\omega C$.

The densities are eliminated from Eq. (3) by means of the Poisson equation. If trap states are present, it is, however, necessary to establish a relationship between the free (n) and trapped (n_t) charge carrier densities. We therefore use the following equation considering the dynamics of trap states [18]:

$$dn_t/dt = c_n(N_t - n_t) - e_n n_t, \tag{4}$$

where e_n and c_n are escape and capture rates, respectively, and N_t is the overall number of trap states (which may be distributed in energy). The ratio e_n/c_n is obtained from an examination of detailed balance in the steady state ($dn_t/dt = 0$). For an exponential energetic distribution of trap states [$h(E) = N_t/E_t \cdot \exp(-E/E_t)$] and assuming $c_n = \sigma\langle v_{\mathrm{th}}\rangle n$, with σ being the trap capture cross section and $\langle v_{\mathrm{th}}\rangle$ the average thermal velocity of carriers, one can define the typical trapping time $\tau_{\mathrm{trap}} = (\sigma\langle v_{\mathrm{th}}\rangle N_t)^{-1}$ and obtains the ac parts of the charge carrier densities in the small signal approximation:

$$\hat{n}_{t,\mathrm{ac}} = \hat{n}_{\mathrm{ac}}\frac{1/l}{i\omega\tau_{\mathrm{trap}} + \Theta(x)}. \tag{5}$$

Therein $\Theta(x) = n_{\mathrm{dc}}(x)/n_{t,\mathrm{dc}}(x)$ is the position-dependent ratio of the free and trapped steady-state charge carrier densities and $l = E_t/k_BT$, where E_t characterizes the depth of the exponential trap distribution as given above. Now one can eliminate the charge carrier densities in Eq. (3) and thus obtain an inhomogeneous first-order linear differential equation in F_{ac} which can directly be integrated numerically to obtain the complex admittance which is the experimental observable.

Finally, in order to account for the disordered nature of transport, a broad distribution of transit times $P(\log\tau_{\mathrm{tr}})d\log\tau_{\mathrm{tr}}$ has to be taken into account additionally [14]. However, as the set of equations cannot be solved analytically with trap states and a field-dependent mobility, we have chosen a different but equivalent approach by considering a distribution of zero-field mobilities $P(\log\mu_0)d\log\mu_0$ being proportional to $-P(\log\tau_{\mathrm{tr}}) \times d\log\tau_{\mathrm{tr}}$. The calculation then has to be carried out for different values of μ_0 and the admittance has to be averaged according to $P(\log\mu_0)$. This results in smearing the signal over a larger range of frequencies as it would be for one single value of μ_0. In contrast to Martens *et al.* we have chosen a Gaussian distribution for $P(\log\mu_0)$ (with a width σ_μ on a decimal log scale) as this seems to be more realistic than the rectangular one used in [14].

The devices under investigation consisted of a vacuum-deposited Alq_3 film sandwiched between aluminum and calcium electrodes as anode and cathode, respectively. For further details of the device preparation we refer to [17]. The measurements of the complex impedance were carried out in a cryostat under nitrogen atmosphere. The measurement system consisted of a frequency response analyzer (Solartron SI 1260) and a broadband dielectric converter (Novocontrol BDC).

Figure 1 shows data of the conductance G and the capacitance C of a 215 nm thick Alq_3 film for different values of the applied dc bias. At zero bias the low-frequency conductance is very low (close to the limits of the instrument) and the capacitance is frequency independent and equal to the geometrical value $C = \varepsilon_r\varepsilon_0 A/d$ (with $\varepsilon_r \approx 4$), as expected for an insulating dielectric. However, as the bias is increased well above the built-in voltage ($V_{\mathrm{bi}} \approx 1$ V) the behavior changes drastically due to carrier injection. The capacitance now shows a minimum at a distinct frequency, which is shifted to higher values as the bias increases, and additionally C strongly increases towards lower frequency. While the latter is an indication of dispersive transport and determines the dispersion parameter α, the position of the inflection point [f_{tr} as indicated by arrows in Fig. 1 (bottom)] is determined by the average carrier transit time. The shape of $G(\omega)$ and $C(\omega)$ is qualitatively similar to the ones reported on PPV in Ref. [14]; however, in the case of Alq_3 one has to consider the strong field dependence of the dc mobility and trapping in distributed trap states. The former leads to the observed strong shift of f_{tr} by almost 2 orders of magnitude between 5 and 10 V, while the latter is responsible for the rapid increase of the conductance with applied bias.

The data in Fig. 1 have been analyzed with the numerical procedure presented above to determine the dispersion parameters (M, α, σ_μ). The parameters describing the dc behavior (trap energy E_t and density N_t, zero-field mobility μ_0 and field enhancement factor β) were extracted from independently measured steady-state I-V characteristics as described elsewhere [17]. The results of the simulation for different dc bias values are included as solid lines in Fig. 1. For bias values between 4 and 10 V the dispersion parameter α varied between 0.40 and 0.46, M between 0.28 and 0.17, and σ_μ between 1.02 and 0.98. The latter indicates a broad distribution of transit times spread over more than two decades. The used value of $\sigma\langle v_{\mathrm{th}}\rangle$ describing the trap dynamics was 10^{-13} cm^3/s. However, it turned out that this parameter

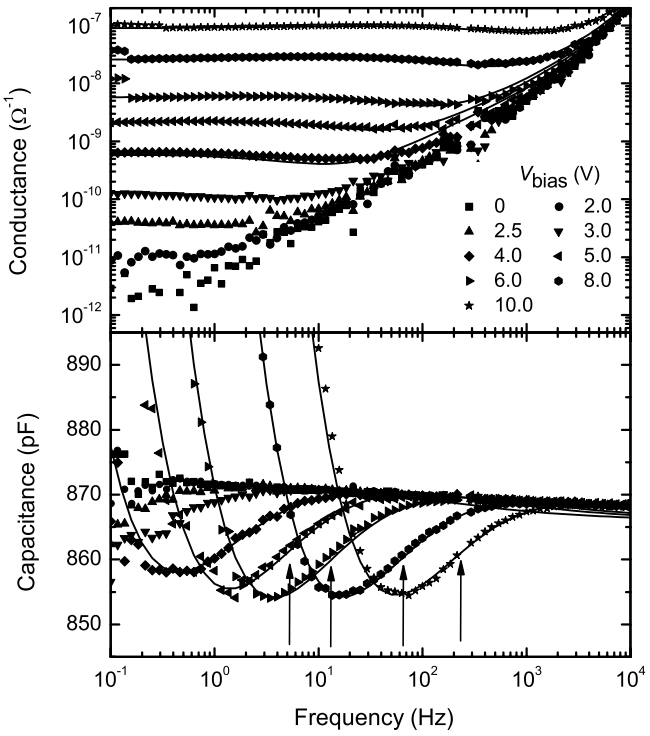

FIG. 1. Frequency-dependent conductance G (top) and capacitance C (bottom) for different bias of an Alq_3/Ca device with a 215 nm thick Alq_3 layer measured at 218 K. The arrows indicate the transit frequency for each bias. Lines are simulations according to our SCLC model.

has comparatively little influence on the shape of the simulated curves since the trap dynamics is much faster than the time scale investigated here. The comparison of the simulated curves with the experimental data in Fig. 1 shows that the presented model accurately describes the ac behavior of injected electrons in Alq_3. We have also performed this analysis for different temperatures (see the inset in Fig. 3) and on a 350 nm thick sample (not shown). Values of the dispersion parameter α were found in the range between 0.4 and 0.5 comparable to the ones obtained on PPV [14]. However, the distribution of transit times is much broader in Alq_3, which might be related to the stronger field dependence of the mobility as compared to PPV [19].

A characteristic feature of dispersive transport is the so-called universality of the photocurrent transients: if plotted in a normalized way as $I(t)/I(\tau_{tr})$ vs t/τ_{tr} experimentally observed transients have the same shape for different electric fields (see, e.g., [20]). In our case we can make a similar representation by normalizing C and the ac part of the conductance $G_{ac}/\omega = [G(\omega) - G(\omega \rightarrow 0)]/\omega$ with respect to the transit frequency f_{tr}. As shown in Fig. 2 the curves for different bias values all have the same shape which again reflects the dispersive nature of electron transport in Alq_3.

There remains an important parameter to be investigated, namely, the temperature dependence. It has been

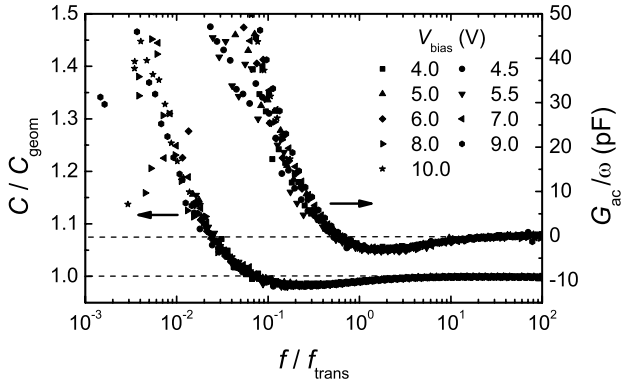

FIG. 2. Normalized representation of C and G_{ac}/ω from Fig. 1 showing the time scale invariance of the curves for different bias values.

demonstrated already in an earlier paper that the dc mobility shows a pronounced temperature dependence following an empirical Poole-Frenkel law [17]. Thus it is not unexpected that for a given bias value the minimum in the capacitance shifts to lower frequency with decreasing temperature (see the inset of Fig. 3). However, it is astonishing that the shape of the curves in the normalized representation of Fig. 3 and consequently the values of the dispersion parameter α almost do not change with temperature. This can be seen as a strong indication for charge carrier transport in Alq_3 being dominated by positional (off-diagonal) disorder.

There have been several models proposed to describe dispersive transport in disordered organic solids (for reviews, see, e.g., [16,20]). Of these, the formalism by Scher and Montroll [21], multiple trapping arguments [22], and disorder models [23,24] have been the most-widely used. We will not discuss the properties of these models in detail here; however, from the observed independence of the dispersivity on temperature we can clearly rule out multiple trapping models as they rely on energetic

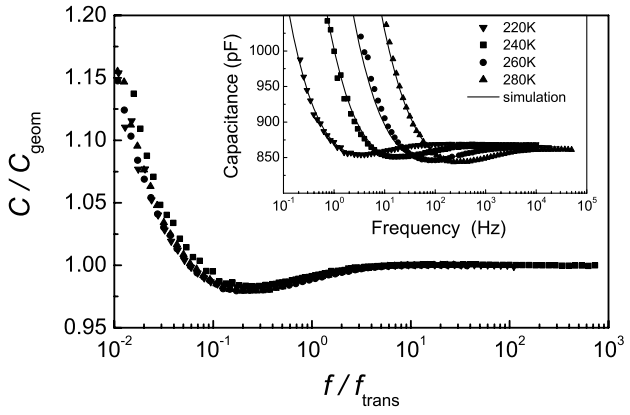

FIG. 3. Frequency-dependent capacitance C for different temperatures measured at a bias voltage of 6 V (inset) and normalized representation of C showing the temperature invariance of the curves.

(diagonal) disorder. In particular, for an exponential distribution of trap states being characterized by a trap energy $E_t = k_B T_t$ one would expect a temperature-dependent dispersion parameter $\alpha \propto T/T_t$, which is clearly not observed here. On the other hand, investigations of steady-state I-V characteristics of Alq_3 electron-only devices have revealed that traps distributed in energy (with E_t in the range 0.11–0.15 eV) play an important role in the behavior of these devices [8,10,17]. Thus we have to conclude that trapping of charge carriers and hopping due to disorder act independently in this material. This is understandable, since typical trap densities of about 10^{17} cm^{-3} as obtained by our work [17] and others [8,9] imply that there is a trap at roughly every twentieth molecule, whereas hopping usually occurs between next-neighbor molecules having a density of approximately 10^{21} cm^{-3}.

Our analysis also gives detailed information about the temperature and field dependence of charge carrier dynamics in Alq_3. As already mentioned, neither the dispersion parameter α nor the parameter σ_μ characterizing the distribution of transit times shows a significant dependence on temperature or electric field; however, a strong T and F dependence is observed for the mean value of the distribution function which corresponds to the dc mobility. We find that the latter follows a Poole-Frenkel–like behavior $\mu_{dc} = \mu_0 \exp(\beta\sqrt{F})$ with parameters μ_0 and β depending on the temperature (see also [17]). The widely accepted description of such a behavior is by disorder models [23,24]. However, without going into details we can say that these models cannot describe our experimental findings, as, for example, the temperature dependence of the zero-field mobility μ_0 follows an Arrhenius law, whereas disorder models predict a much stronger temperature dependence [$\log(\mu_0) \propto T^{-2}$ [23], respectively, $\propto T^{-3/2}$ [24]]. The reason for this discrepancy might be found in the used Miller-Abrahams–type hopping transfer rates which are based on hydrogenlike wave functions with spherical symmetry. Given the geometry of the Alq_3 molecule with the three quinoline ligands pointing into different directions one can easily imagine that the hopping rates of charge carriers between neighboring molecules depend critically on the mutual orientation of these molecules. Thus in a more sophisticated treatment one should include also rotational degrees of freedom for the Alq_3 molecule which we assume to be the source of the off-diagonal disorder.

In conclusion we have shown that impedance spectroscopy under SCLC conditions is a powerful tool to study the dynamics of charge carriers in disordered organic semiconductors even in the very general case of a field-dependent mobility and the presence of trap states. The application of this approach to Alq_3 has revealed dispersive electron transport with a broad distribution of transit times. The identification of off-diagonal disorder as the dominant mechanism shows that charge carrier trapping and hopping are independent features in this material.

We thank M. Schwoerer and A. G. Mückl for helpful discussions and the Deutsche Forschungsgemeinschaft for financial support.

*Present address: Experimental Physics IV, University of Augsburg, 86135 Augsburg, Germany.
Electronic address: Wolfgang.Bruetting@physik.uni-augsburg.de

[1] C. Tang and S. VanSlyke, Appl. Phys. Lett. **51**, 913 (1987).
[2] A. Ioannidis, E. Forsythe, Y. Gao, M. Wu, and E. Conwell, Appl. Phys. Lett. **72**, 3038 (1998).
[3] S. Barth, P. Müller, H. Riel, P. Seidler, W. Rieß, H. Vestweber, and H. Bässler, J. Appl. Phys. **89**, 3711 (2001).
[4] R. Kepler, P. Beeson, S. Jacobs, R. Anderson, M. Sinclair, V. Valencia, and P. Cahill, Appl. Phys. Lett. **66**, 3618 (1995).
[5] T. Tsutsui, H. Tokuhisa, and M. Era, Proc. SPIE Int. Soc. Opt. Eng. **3281**, 230 (1998).
[6] B. Chen, W. Lai, Z. Gao, C. Lee, S. Lee, and W. Gambling, Appl. Phys. Lett. **75**, 4010 (1999).
[7] G. G. Malliaras, Y. Shen, D. H. Dunlap, H. Murata, and Z. H. Kafafi, Appl. Phys. Lett. **79**, 2582 (2001).
[8] M. Stößel, J. Staudigel, F. Steuber, J. Blässing, J. Simmerer, and A. Winnacker, Appl. Phys. Lett. **76**, 115 (2000).
[9] A. Werner, J. Blochwitz, M. Pfeiffer, and K. Leo, J. Appl. Phys. **90**, 123 (2001).
[10] P. Burrows, Z. Shen, V. Bulovic, D. McCarty, S. Forrest, J. Cronin, and M. Thompson, J. Appl. Phys. **79**, 7991 (1996).
[11] E. Silinsh, *Organic Molecular Crystals* (Springer, Berlin, 1980).
[12] M. Pope and C. E. Swenberg, *Electronic Processes in Organic Crystals and Polymers* (Oxford University Press, Oxford, 1999).
[13] J. Shao and G. T. Wright, Solid State Electron. **3**, 291 (1961).
[14] H. Martens, H. Brom, and P. Blom, Phys. Rev. B **60**, R8489 (1999).
[15] M. Lampert and P. Mark, *Current Injection in Solids* (Academic Press, New York, 1970).
[16] H. Böttger and V. Bryksin, *Hopping Conduction in Solids* (VCH Publishers, Inc., Berlin, 1985).
[17] W. Brütting, S. Berleb, and A. Mückl, Org. Electron. **2**, 1 (2001).
[18] P. Blood and J. W. Orton, *The Electrical Characterization of Semiconductors: Majority Carriers and Electron States* (Academic Press, London, 1992).
[19] P. Blom and M. Vissenberg, Phys. Rev. Lett. **80**, 3819 (1998).
[20] P. M. Borsenberger and D. S. Weiss, *Organic Photoreceptors for Imaging Systems* (M. Dekker, New York, 1993).
[21] H. Scher and E. Montroll, Phys. Rev. B **12**, 2455 (1975).
[22] J. Noolandi, Phys. Rev. B **16**, 4474 (1977).
[23] H. Bässler, Phys. Status Solidi B **175**, 15 (1993).
[24] D. Dunlap, P. Parris, and V. Kenkre, Phys. Rev. Lett. **77**, 542 (1996).